1 The generation of HepG2 transmitochondrial cybrids to reveal the role of mitochondrial genotype in
2 idiosyncratic drug-induced liver injury: a translational *in vitro* study
3
4

5 Amy L. Ball[1], Carol E. Jolly[1], Jonathan J. Lyon[2], Ana Alfirevic[3], Amy E. Chadwick[1*]

6 [1] MRC Centre for Drug Safety Science, Department Pharmacology and Therapeutics, University of
7 Liverpool, Liverpool, UK
8 [2.]GSK GlaxoSmithKline, Safety Assessment, Ware, UK
9 [3] The Wolfson Centre for Personalised Medicine, Department Pharmacology and Therapeutics,
10 University of Liverpool, Liverpool, UK
11 *Corresponding Author. E-mail: aemercer@liverpool.ac.uk, Tel: +441517950148.
12 **ORCID ID:** 0000-0002-7399-8655

Abstract

14 Background. Evidence supports an important link between mitochondrial DNA (mtDNA) variation
15 and adverse drug reactions such as idiosyncratic drug-induced liver injury (iDILI). Here we describe
16 the generation of HepG2-derived transmitochondrial cybrids in order to investigate the impact of
17 mtDNA variation upon mitochondrial (dys)function and susceptibility to iDILI against a constant
18 nuclear background. In this study, cybrids were created to contain mitochondrial genotypes of
19 haplogroup H and haplogroup J for comparison.

20 Methods. Briefly, HepG2 cells were depleted of mtDNA to make rho zero cells before the
21 introduction of known mitochondrial genotypes using platelets from healthy volunteers (n=10), thus
22 generating 10 distinct transmitochondrial cybrid cell lines. The mitochondrial function of each was
23 assessed at basal state and following treatment with compounds associated with iDILI; flutamide, 2-
24 hydroxyflutamide and tolcapone, by ATP assays and extracellular flux analysis.

25 Findings. Overall, baseline mitochondrial function was similar between haplogroups H and J.
26 However, haplogroup specific responses to mitotoxic drugs were observed; haplogroup J was more
27 susceptible to the inhibition of respiratory complexes I and II, and also to the effects of tolcapone, an
28 uncoupler of mitochondrial respiration.

29 Conclusions. This study demonstrates that HepG2 transmitochondrial cybrids can be created to
30 contain the mitochondrial genotype of any individual of interest, thus providing a practical and
31 reproducible system to investigate the cellular consequences of variation in mitochondrial genome
32 against a constant nuclear background. Additionally the results support that that inter-individual
33 variation in mitochondrial genotype and haplogroup may be a factor in determining sensitivity to
34 mitochondrial toxicants.

38

Introduction

41 Drug-induced liver injury (DILI) is a leading cause of acute liver failure in the western world (Bernal and Wendon, 2013; Tujios and Lee, 2018). Although it is rare (19.1 cases per 100 000 inhabitants), it is a major cause of drug withdrawal due to its associated morbidity and mortality (Leise et al., 2014). Drug-induced liver injury can be broadly divided into two categories, idiosyncratic and intrinsic injury. Idiosyncratic DILI (iDILI) is characterised by a complex dose-response relationship, lack of predictivity from the primary pharmacology of a drug and significant interindividual variability. This means that despite being less common than intrinsic injury, iDILI can be viewed as far more costly (Fontana, 2014).

49 Drug-induced mitochondrial dysfunction is one of the mechanisms implicated in the onset of DILI, supported by the fact that 50% of drugs with a black box warning for hepatotoxicity also contain a mitochondrial liability, with many of these drugs associated specifically with iDILI (Dykens and Will, 2007). It has been hypothesised that mitochondria is an important source of interindividual variation, underpinning susceptibility to iDILI. Specifically, mitochondria contain multiple copies of their own genome, mitochondrial DNA (mtDNA). Furthermore, single nucleotide polymorphisms (SNPs) in mtDNA are often inherited together forming mitochondrial haplogroups. Not only have associations between specific haplogroups and mitochondrial function been determined, but haplogroups have also been associated with specific adverse drug reactions and drug efficacy (Jones et al., 2021a).

59 The HepG2 cell line is one of the most commonly used preclinical cell lines for the *in vitro* assessment of DILI. However, this homogenous cell line does not encompass interindividual variation, including that of the mitochondrial genome. The importance of assessing the role of interindividual variation on patient susceptibility to adverse drug reactions is well recognised and the identification of mtDNA variants that confer susceptibility to iDILI could prove invaluable in drug development and drug safety. However, given the high economic cost associated with large, multicentre clinical trials, there is a need for new strategies enabling interindividual variation to be accounted for at the preclinical stage (Fermini et al., 2018; Jones et al., 2021b).

67 The generation of transmitochondrial cybrids enables mtDNA variation to be incorporated into reproducible *in vitro* models. Transmitochondrial cybrids are typically produced by the fusion of enucleated cells (cytoplasts) or anucleate cells (e.g. platelets) with cells that have been depleted of their mtDNA (rho zero [ρ0] cells) (King and Attardi, 1989). When cybrids are generated using the same population of ρ0 cells fused with anucleate cells harbouring different mtDNA variants, it is possible for the effects of mtDNA to be assessed against a stable nuclear background (Wilkins et al.,

73   2014; Penman et al., 2020). Excitingly, the representation of mtDNA variation using HepG2
74   transmitochondrial cybrids may offer enhanced preclinical prediction of iDILI by facilitating the *in*
75   *vitro* elucidation of the mechanistic basis of any differences associated with mtDNA variants, yet to-
76   date there have been no reports of the generation of cybrids from a HepG2 p0 cell line (Bale et al.,
77   2014).

78   Therefore, the overall aim of this study was to generate a panel of HepG2 transmitochondrial
79   cybrids, as a proof of principle study, to investigate the effect of mtDNA variants upon mitochondrial
80   function and their role, if any, in conferring susceptibility to drug-induced mitochondrial dysfunction.
81   Specifically, ten populations of HepG2 transmitochondrial cybrids (herein referred to as cybrids)
82   were created and characterised; five using platelets derived from healthy volunteers of haplogroup
83   H and five from haplogroup J. Haplogroup H was selected as it is the most common haplogroup in
84   the UK (Eupedia, 2016). Haplogroup J, on the other hand, is less common but is characterised by
85   non-synonymous mutations in regions of the mitochondrial genome that encode mitochondrial
86   respiratory complex I (Van Oven and Kayser, 2009; Eupedia, 2016). See Figure 1 for a schematic
87   overview of the study.

88   Mitochondrial function was measured by ATP quantification in acutely galactose-conditioned cells,
89   and extracellular flux (XF) analysis of both total respiratory chain function and the function of
90   specific respiratory complexes, in whole and permeabilised cybrids, respectively. Drug-induced
91   mitochondrial dysfunction was assessed by the treatment of cybrids with a panel of compounds
92   selected to comprise of known hepatotoxins (a clinical association with DILI) with proven
93   mitochondrial liabilities; flutamide, 2-hydroxyflutamide and tolcapone, alongside structural
94   counterparts which are not hepatotoxic; bicalutamide and entacapone. Flutamide, a non-steroidal
95   antiandrogen for the treatment of prostate cancer has a boxed warning for hepatotoxicity and is a
96   known inhibitor of mitochondrial complex I (Coe et al., 2007). 2-hydroxyflutamide, is the primary
97   metabolite of flutamide and is a known inhibitor of both respiratory complex I and respiratory
98   complex II. In humans, the rapid first-pass metabolism of flutamide results in 2-hydroxyflutamide
99   having a much higher maximum serum concentration than its parent compound (4400 nM versus
100 72.2 nM). However, HepG2 cells have limited expression of many enzymes required for xenobiotic
101 metabolism, including cytochrome P450 1A2, the primary route of flutamide metabolism to
102 generate 2-hydroxyflutamide; therefore cybrids were also dosed with 2-hydroxyflutamide directly
103 (Shet et al., 1997; Sison-Young et al., 2015; Ball et al., 2016). Tolcapone, a catechol-o-methyl
104 transferase inhibitor used to treat Parkinson's disease was withdrawn due to cases of liver failure
105 and is a known uncoupler of oxidative phosphorylation (Olanow, 2000; Benabou and Waters, 2003;
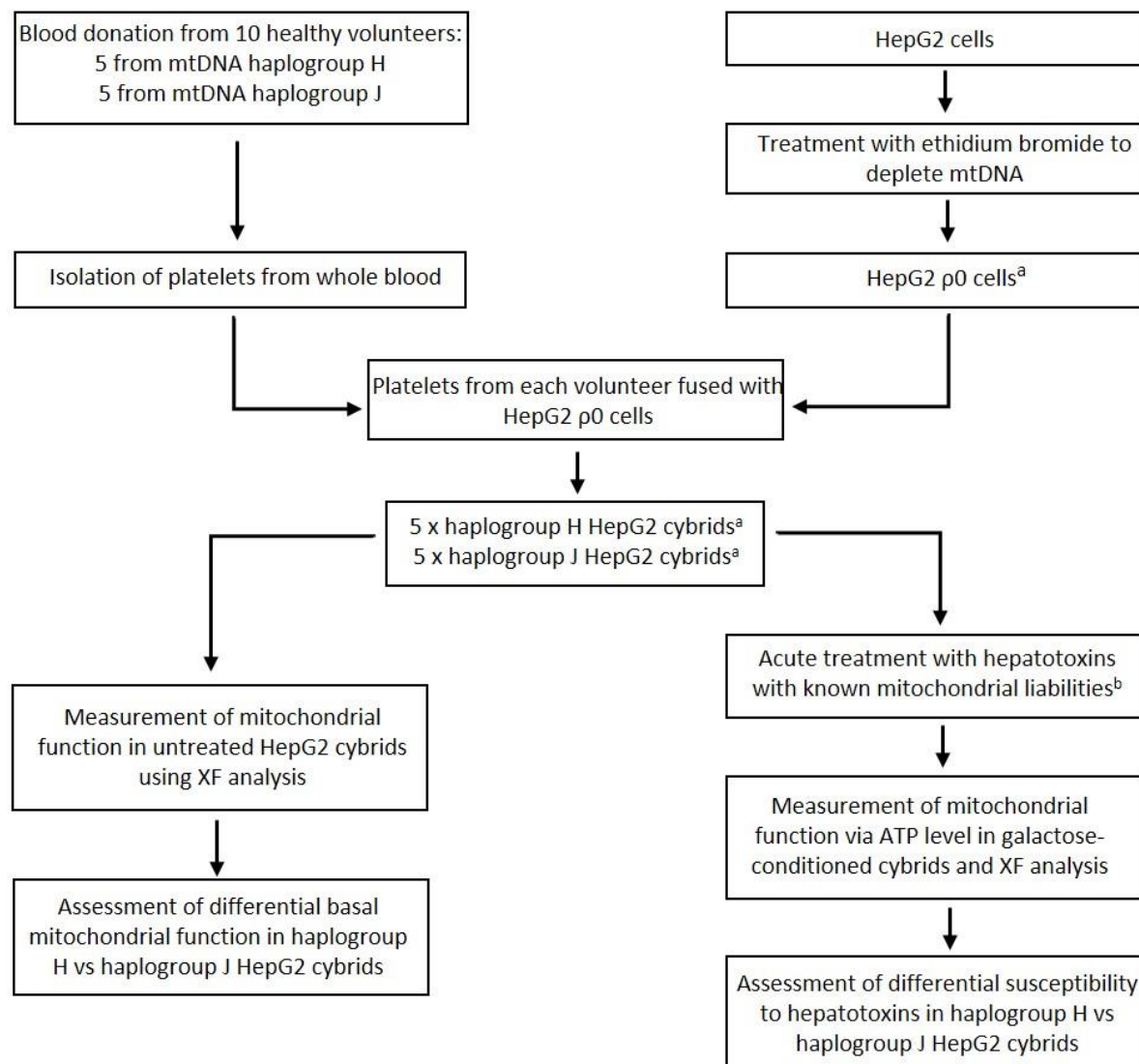106 Olanow and Watkins, 2007).

4

107

Figure 1 Study Overview.

[a] HepG2 ρ0 cells were characterised to ensure the complete depletion of mtDNA and HepG2 cybrids were characterised to ensure the expression of mtDNA-encoded proteins. Methods of characterisation are described in the Supplementary Information.

[b] Flutamide, 2-hydroxyflutamide and tolcapone, alongside non-hepatotoxic structural counterparts; bicalutamide and entacapone.

Abbreviations: Abbreviations: mtDNA, mitochondrial DNA; ρ0, rho zero; XF, extracellular flux.

117 Results

118 *Haplogroup J cybrids have greater respiratory complex activity than haplogroup H cybrids*

119 Assessment of basal mitochondrial function using a mitochondrial stress test showed no significant

120 difference between haplogroup H and J cybrids in multiple parameters of mitochondrial respiration

121 (Figure 2A). Contrastingly, haplogroup J cybrids had significantly greater ($\geq$2 fold; p=0.025, p=0.001)

122 complex I and II-driven maximal respiration (herein referred to as complex activity for clarity)
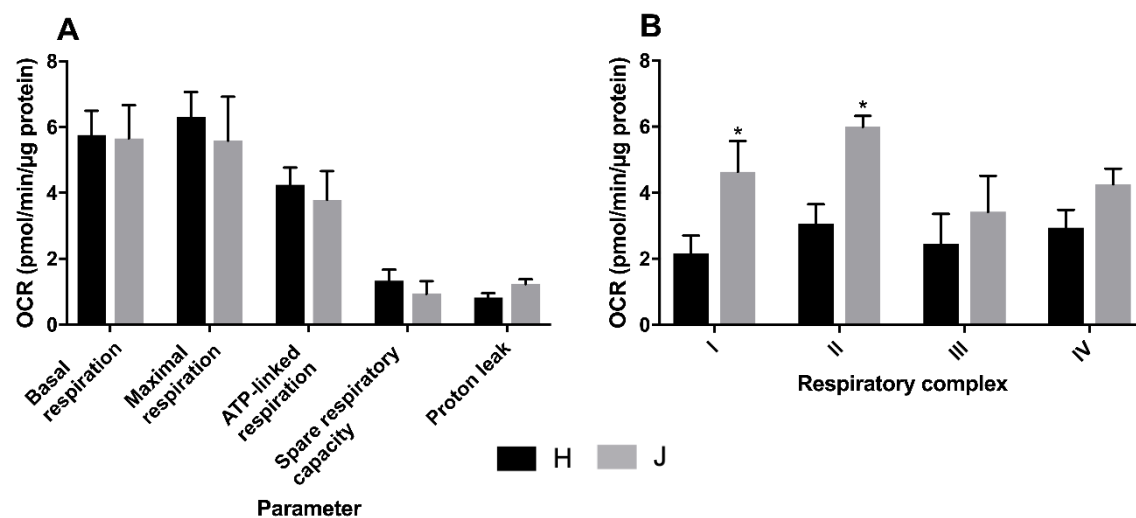
123 (Figure 2B).

Figure 2 **Basal mitochondrial function and respiratory complex activity in haplogroup H and J HepG2 cybrids.**
A: Untreated haplogroup H and J cybrids were assessed using extracellular flux analysis and a mitochondrial stress test to measure: basal respiration, maximal respiration, ATP-linked respiration, spare respiratory capacity and proton leak. **B:** Untreated haplogroup H and J cybrids were assessed using extracellular flux analysis and respiration was stimulated by the supply of respiratory complex-specific substrates. Complex I-IV activity was defined as complex I-IV driven maximal respiration. Statistical significance between haplogroup H and J cybrids: * *p*<0.05. Data are presented as mean + SEM of n=5 experiments. Abbreviations: OCR, oxygen consumption rate. Source data: fig2 – source data file.xslx

124

125 *Inhibition of mitochondrial respiration by flutamide is similar in haplogroup H and J cybrids*

7

126   Acute treatment of galactose-conditioned cybrids with flutamide did not induce cytotoxicity (i.e. no

127   significant lactate dehydrogenase [LDH] release) at any of the concentrations used (data not shown).

128   A substantial, concentration-dependent decrease in ATP was evident when cybrids were treated

129   with ≥33 μM flutamide, but the decrease was not significantly different between haplogroup H and J

130   cybrids (Figure 3A). Concordantly, there was no significant difference in the ATP level EC_{50} between

131   the two haplogroups. XF analysis also revealed no significant difference in parameters of

132   mitochondrial respiration between haplogroup H and haplogroup J cybrids when treated with

133   flutamide, though haplogroup J cybrids did have a greater proton leak and reduced spare respiratory
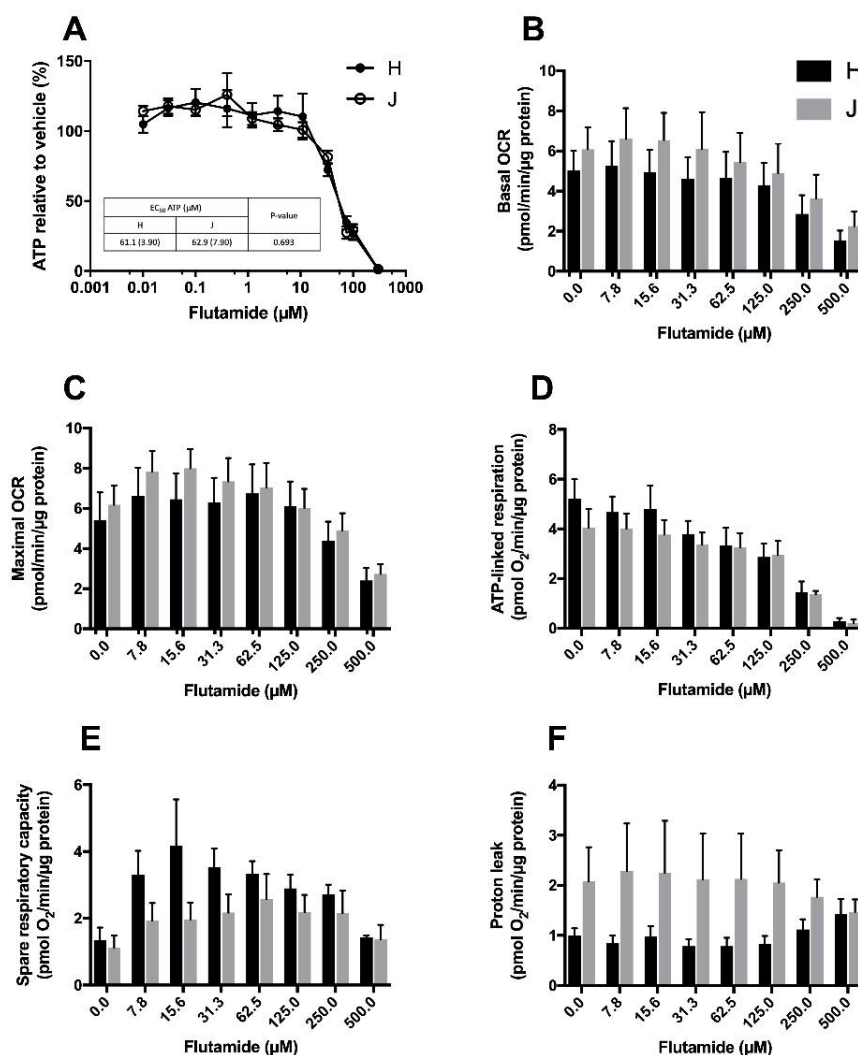

Figure 3 The effect of flutamide upon ATP levels and mitochondrial respiratory function in haplogroup H and J HepG2 cybrids. A: Cybrids were treated (2 h) with up to 300 μM flutamide in galactose medium. ATP values are expressed as a percentage of those of the vehicle control. B-F: Changes in basal respiration, maximal respiration, ATP-linked respiration, spare respiratory capacity and proton leak following acute treatment with flutamide (up to 500 μM). Data are presented as mean ± SEM of n=5 experiments. Abbreviations: OCR, oxygen consumption rate. Source data: fig3 – source data file.xslx

134   capacity than haplogroup H at all concentrations, but this was not significant (Figure 3B-F).

135   *Inhibition of mitochondrial respiration by 2-hydroxyflutamide is similar in haplogroup H and J cybrids*

136   Acute treatment of galactose-conditioned cybrids with 2-hydroxyflutamide did not induce

137   cytotoxicity at any of the concentrations used (data not shown). A substantial, concentration-

138   dependent decrease in ATP level was evident when cybrids were treated with ≥33 µM 2-

139   hydroxyflutamide, but the decrease was not significantly different between haplogroup H and J

140   cybrids at any single concentration (Figure 4A); however, a comparison of EC_{50} values showed a

141   small but significantly lower EC_{50} value in haplogroup H cybrids (Figure 4A; p=0.003). XF analysis also

142   revealed no significant difference in parameters of mitochondrial respiration between haplogroup H

143   and haplogroup J cybrids when treated with 2-hydroxyflutamide (Figure 4B-F). As was the case with

144   flutamide, 2-hydroxyflutamide-treated haplogroup J cybrids had a greater proton leak and reduced

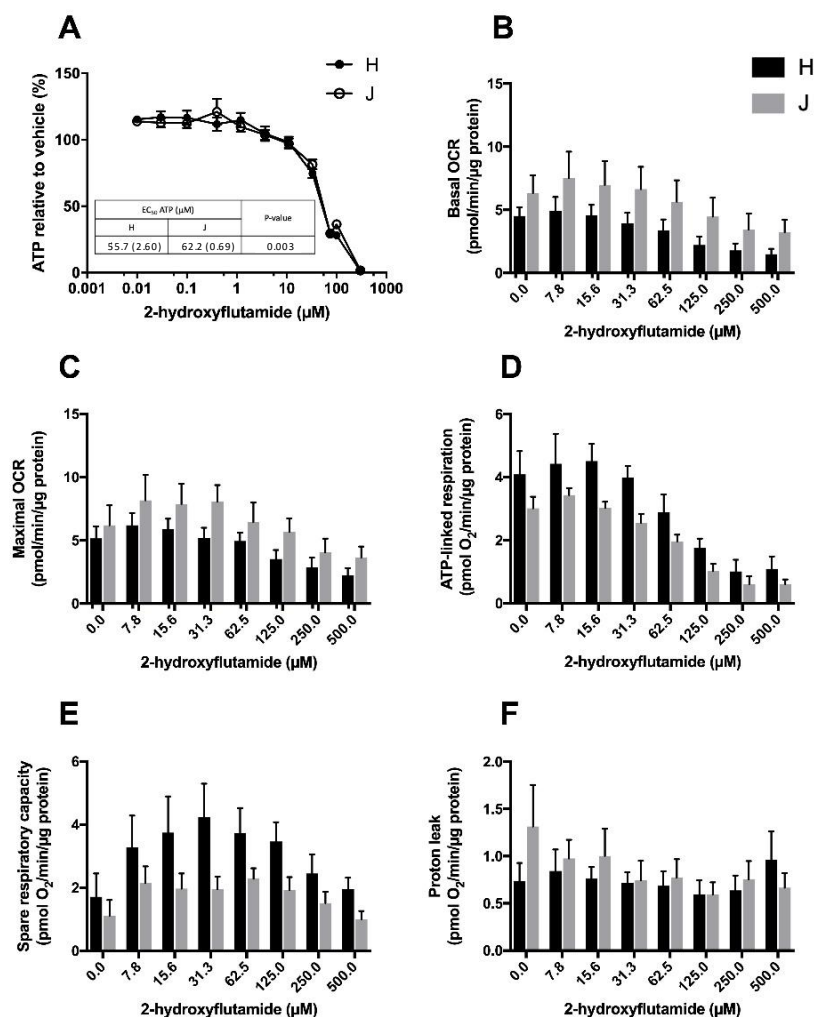145   spare respiratory capacity compared with haplogroup H at most concentrations, but this was not

Figure 4 The effect of 2-hydroxyflutamide upon ATP levels and mitochondrial respiratory function in haplogroup H and J HepG2 cybrids. A: Cybrids were treated (2 h) with up to 300 µM 2-hydroxyflutamide in galactose medium. ATP values are expressed as a percentage of those of the vehicle control. **B-F:** Changes in basal respiration, maximal respiration, ATP-linked respiration, spare respiratory capacity and proton leak following acute treatment with 2-hydroxyflutamide (up to 500 µM). Data are presented as mean ± SEM of n=5 experiments. Abbreviations: OCR, oxygen consumption rate. Source data: fig4 – source data file.xslx

146   significant (Figure 4E, F).

147   *Haplogroup H cybrids are resistant to tolcapone-induced ATP depletion at <75 µM*

148   Cellular ATP levels following treatment with up to 75 µM tolcapone were significantly higher in

149   haplogroup H cybrids; this was reflected by the significantly higher EC_{50} in haplogroup H cybrids,

150   almost twice that of haplogroup J (Figure 5A; p<0.0001). At higher concentrations of tolcapone

151   however, there was no significant difference between the two haplogroups (Figure 5A). XF analysis

152   showed no significant difference in parameters of mitochondrial respiration between haplogroup H

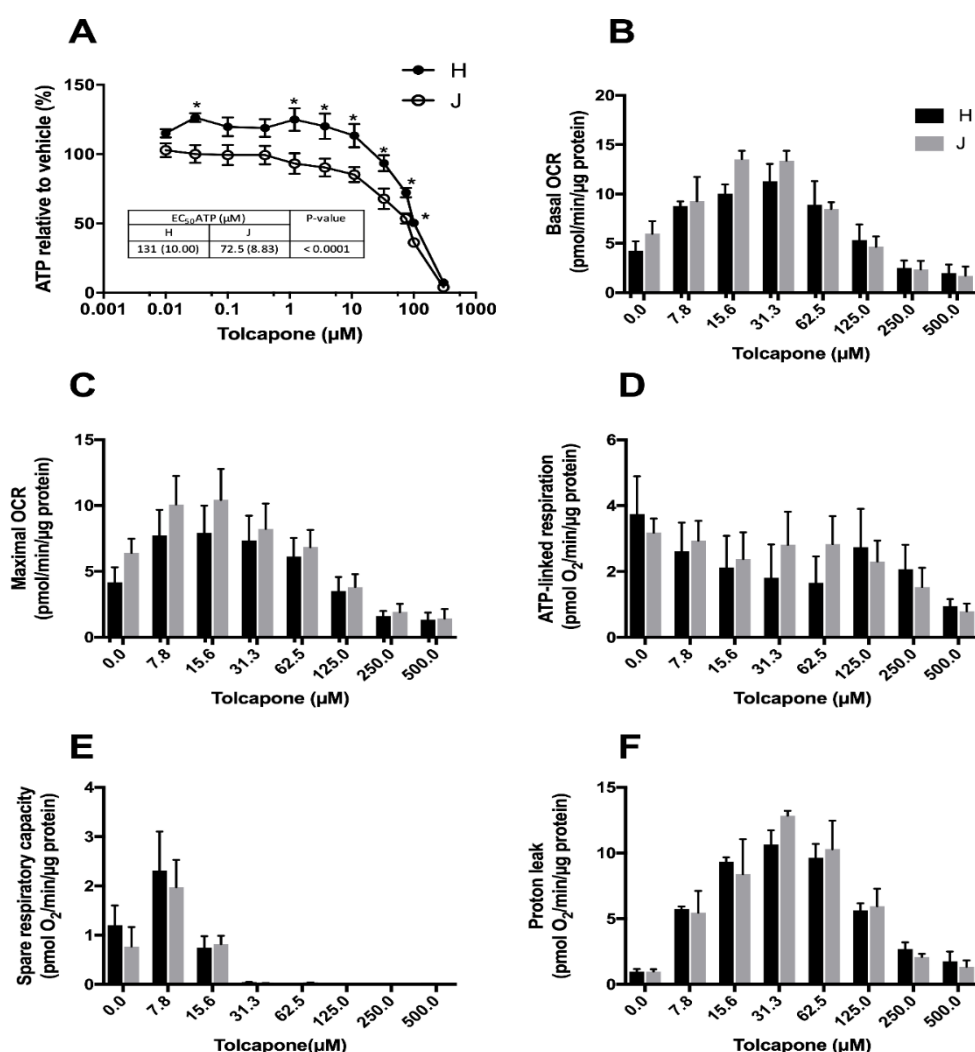153   and haplogroup J cybrids when treated with tolcapone (Figure 5B-F).

Figure 5 The effect of tolcapone upon ATP levels and mitochondrial respiratory function in haplogroup H and J HepG2 cybrids. A: Cybrids were treated (2 h) with up to 300 µM tolcapone in galactose medium. ATP values are expressed as a percentage of those of the vehicle control. **B-F:** Changes in basal respiration, maximal respiration, ATP-linked respiration, spare respiratory capacity and proton leak following acute treatment with tolcapone (up to 500 µM). Statistical significance between : haplogroup H and J cybrids* *p*<0.05. Data are presented as mean ± SEM of n=5 experiments. Abbreviations: OCR, oxygen consumption rate. Source data: fig 5 – source data file.xslx

154

155 *Haplogroup J cybrids have greater respiratory complex activity but are more susceptible to inhibition of*
156 *complex I and II activity by flutamide and 2-hydroxyflutamide*

157 When treated with flutamide (complex I inhibitor) haplogroup J cybrids had significantly greater

158 respiratory complex I/II activity at all but the highest flutamide concentration (250 µM), peaking at

159 approximately two-fold greater activity than haplogroup H cybrids (Figure 6A, B). Though complex I

160 activity was greater in haplogroup J cybrids at all concentrations, haplogroup J cybrids exhibited a

161 bigger decrease (compared with haplogroup H cybrids) in complex I activity relative to control when

162 treated with flutamide (Figure 6A). The effect of treatment with 2-hydroxyflutamide mirrored the

163 effect of its parent compound, flutamide, with greater complex I activity in haplogroup J cybrids at

164 all concentrations, but with haplogroup J cybrids exhibiting the biggest decrease in complex I activity

165 relative to control (Figure 6C).

166 A smaller difference was observed in complex II activity between the two cybrid haplogroups when

167 treated with 2-hydroxyflutamide, though greater activity was still evident in haplogroup J cybrids at
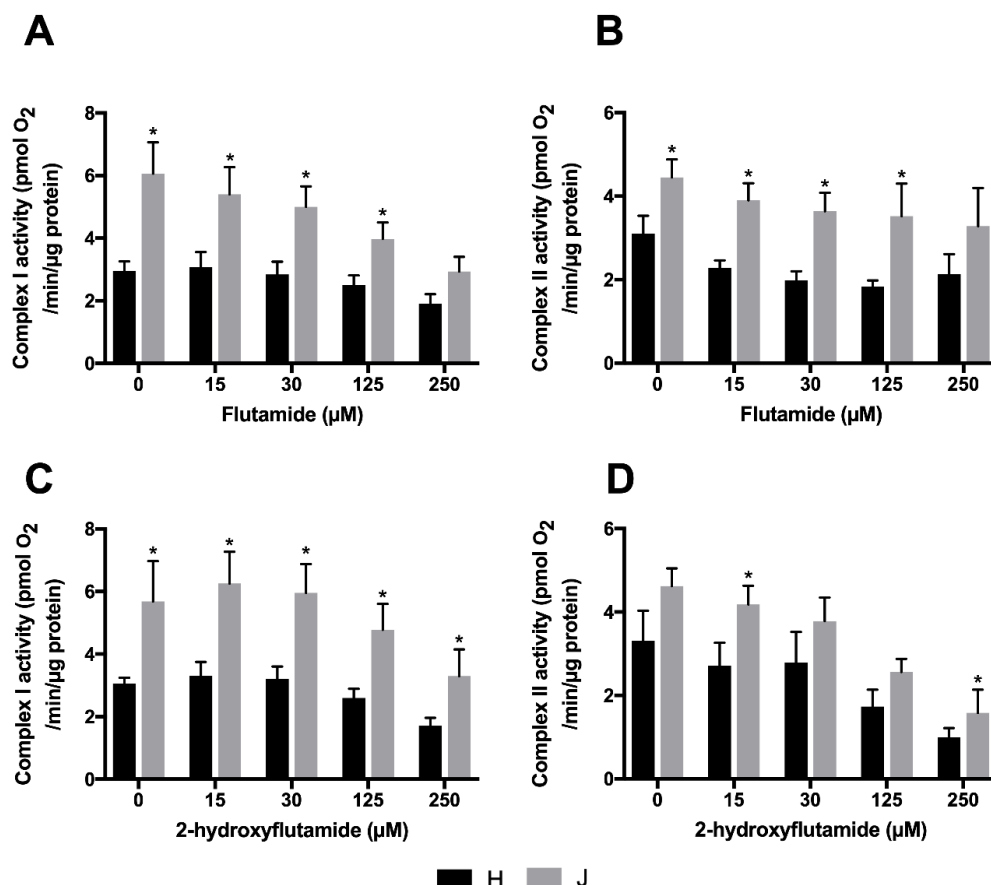
168 all concentrations (Figure 6D).

Figure 6 The effect of flutamide and 2-hydroxyflutamide upon respiratory complex I and II in haplogroup H and J HepG2 cybrids. Permeabilised cybrids were acutely treated with flutamide (**A, B**) or 2-hydroxyflutamide (**C, D**) (≤250 µM) before a mitochondrial stress test using extracellular flux analysis. Complex I/II activity was defined as complex I/II driven maximal respiration. Statistical significance between haplogroup H and J cybrids: * $p < 0.05$. Data are presented as mean + SEM of n=5 experiments. Source data: fig 6 – source data file.xslx

169

The impact of bicalutamide and entacapone on mitochondrial respiration and ATP levels is similar in haplogroup H and J cybrids

When treated with bicalutamide and entacapone (non-hepatotoxic structural counterparts of flutamide and tolcapone, respectively), the effect on mitochondrial respiration and ATP levels was similar in haplogroup H and J cybrids. Full results are described in the Supplementary Information.

Discussion

It has been widely hypothesised that individual variation in mtDNA may be a factor underlying the onset of idiosyncratic adverse drug reactions by drugs known to contain mitochondrial liabilities. Evidence from clinical studies has demonstrated that such associations between mitochondrial genotype and drug efficacy or adverse events do exist (Jones et al., 2021a). However, there is a lack of knowledge and understanding of the importance of these findings due to the presence of nuclear heterogeneity alongside environmental factors in clinical cohorts and the small size of test cohorts, as well as historical limitations in sequencing technology. Because of this we have created a transmitochondrial cybrid cell panel, in which mitochondria of known genotype, sourced from volunteer platelets, were inserted into HepG2 ρ0 cells in order to produce a "personalised model" model of mitotoxicity suitable for mechanistic investigations.

Here we describe the successful generation of 10 distinct transmitochondrial cybrid cell lines, derived from five haplogroup H volunteers and five haplogroup J volunteers. To the best of our knowledge, this is the first time that the creation of a panel of HepG2-derived transmitochondrial cybrids has been reported. Importantly, the HepG2 cell line is one of the most commonly used cell lines in preclinical drug safety testing and therefore the HepG2 cybrids generated in the present study are of great value in improving the understanding of iDILI by providing an *in vitro* representation of the interindividual variation that underpins this adverse drug reaction (Bale et al., 2014). In this work, the utility of these cells to investigate interhaplogroup differences in mitochondrial function has been demonstrated, with HepG2 cybrids of haplogroup J displaying greater mitochondrial respiratory complex activity at basal state. Moreover, our investigations revealed that there were haplogroup-specific differences in susceptibility to hepatotoxic compounds that target the electron transport chain (ETC). Specifically, haplogroup J cybrids were more susceptible to: a reduction in respiratory complex I activity induced by flutamide, a reduction in respiratory complex I and II activity induced by 2-hydroxyflutamide, and a reduction in ATP levels induced by tolcapone.

13

202 The methodology developed for the generation of HepG2 cybrids has enabled the creation of a

203 HepG2 cybrid cell panel from two of the most common mitochondrial haplogroups in England, H and

204 J; which account for more than 50% of the population (Eupedia, 2016). Although baseline

205 assessments revealed only marginal differences in mitochondrial function between haplogroup H

206 and J cybrids, the recruitment of healthy volunteers for this study (i.e. no clinical phenotype of

207 mitochondrial dysfunction), meant that the absence of any substantial differences in mitochondrial

208 function was expected. This recruitment of healthy volunteers is representative of the clinical

209 situation, as individuals who experience iDILI tend not to display a phenotype of mitochondrial

210 dysfunction prior to treatment. Additionally, it should be noted that these results were analysed on

211 the basis of macro-haplogroup (i.e H, J). However, each cybrid cell line has been identified as a

212 separate sub-haplogroup (e.g. H1, J2), based upon the accumulation of specific SNPs (see

213 Supplementary Information). This lack of homogeneity within the test groups may mask

214 associations.

215 The cybrid cell panel was interrogated using known drug mitotoxicants which elicit different effects

216 on the ETC; flutamide and 2-hydroxyflutamide, direct ETC inhibitors, and tolcapone, an ETC

217 uncoupler. The impact of flutamide (complex I inhibitor) and 2-hydroxyflutamide (complex I and II

218 inhibitor) upon cellular ATP level was similar between haplogroup H and J cybrids. However,

219 haplogroup H cybrids exhibited a degree of resistance to ATP depletion induced by tolcapone; a

220 resistance that was not observed in haplogroup J cybrids. This agrees with findings reported by

221 Ghelli *et al.,* 2009 in which a cybrid model (non-hepatic) was used to determine that haplogroup J (vs

222 haplogroups H and U) was more susceptible to uncoupling by the neurotoxic metabolite, 2,5-

223 hexanediol (Ghelli et al., 2009). When assessing the relevance of the results from the present study,

224 it is important to note that test concentrations were selected in order to generate the maximum

225 effect on mitochondrial function in the absence of toxicity. The authors recognise that higher

226 concentrations were used than C_{max} of compounds, however the goal was to model the

227 mitochondrial toxicity experienced in a small number of individuals, which was not possible at lower

228 concentrations. It is important to note that there was a lack of these described haplogroup-specific

229 effects when using the non-hepatotoxic counterparts of the test compounds, bicalutamide and

230 entacapone, illustrating that any differences are mechanisms- via induced mitochondria dysfunction.

231 Further analysis of the effects of the compounds upon respiration showed that the impact of

232 flutamide and 2-hydroxyflutamide on parameters of mitochondrial respiration was similar between

233 haplogroup H and J, though haplogroup J cybrids had consistently higher rates of respiration.

234 Parameters of mitochondrial respiration also remained similar between the two cybrid haplogroups

235 upon treatment with tolcapone. Given that the ATP level of cells, and indeed overall respiration, is

14

236 the product of a myriad of processes to maintain energy status, mitochondrial function was
237 dissected further by assessing the basal activity of specific respiratory complexes. Despite marginal
238 differences in overall basal mitochondrial respiration, the basal activity of specific respiratory
239 complexes showed significantly higher complex I and II activity in haplogroup J compared with
240 haplogroup H cybrids. However, haplogroup J cybrids also displayed a heightened susceptibility to
241 inhibition of complex I and II activity by flutamide/2-hydroxyflutamide. In contrast to complex I,
242 complex II is entirely encoded in the nuclear genome, therefore one might predict that this should
243 not differ between mitochondrial haplogroups. Nonetheless, upon the introduction of the foreign
244 mitochondrial genome into cybrids, the initiation of retrograde responses to the nucleus must
245 ensue, primarily via calcium signalling, which would enable regulation of the nuclear-encoded
246 mitochondrial proteome and potentially enhanced biogenesis of respiratory complexes in
247 haplogroup J (Luo et al., 1997; Amuthan et al., 2002; Srinivasan et al., 2015). This mechanism could
248 account for the observed differential complex II activity.

249 The finding that haplogroup H cybrids are more resistant to ATP depletion induced by tolcapone
250 offers new insights into the potential mechanisms underlying the onset of iDILI in certain individuals.
251 In the case of tolcapone, four instances of liver failure among the 100 000 individuals who were
252 administered the drug led to a black box warning and a switch in use to an alternative in-class
253 compound, entacapone. However, as entacapone has been reported to be less efficacious than
254 tolcapone, the ability to stratify therapy based upon the risk of iDILI, would be of great value (Rivest
255 et al., 1999; Olanow, 2000; Watkins, 2000; Benabou and Waters, 2003; Olanow and Watkins, 2007;
256 Lees, 2008; Longo et al., 2016).

257 Overall, this research offers insights into the potential importance of mitochondrial haplogroup on
258 drug-induced mitochondrial dysfunction and iDILI. In the present study, HepG2 cybrids have been
259 generated from only two mitochondrial haplogroups due to sample size limitations, but the method
260 established offers itself to the generation of HepG2 cybrids from volunteers of other mitochondrial
261 haplogroups and also from volunteers who are identical at the level of subhaplogroup. Furthermore,
262 it is of note that differences in susceptibility have been observed despite the division of cybrids into
263 two haplogroups which encompass much variation, and suggests that the comparison of more
264 homogenous mtDNA subhaplogroups may provide further, more valuable insights into the
265 differences conferred by differential mitochondrial background.

266

267 In conclusion, this study has established a novel, *in vitro* model that provides a preclinical
268 representation of interindividual variation underpinning iDILI, thereby offering much greater
269 translatability to clinical scenarios compared with current, homogenous preclinical models. This is

15

270   paramount in understanding the safety of a drug in a range of populations prior to clinical trials, thus

271   improving patient safety, as well as reducing drug attrition.

272   ## Materials and Methods

273   *Materials*

274   All forms of DMEM were purchased from Life Technologies (Paisley, UK). HepG2 cells were

275   purchased from European Collection of Cell Cultures (Salisbury, UK). Cytotoxicity detection kits were

276   purchased from Roche Diagnostics Ltd (West Sussex, UK). Clear and white 96-well plates were

277   purchased from Fisher Scientific (Loughborough, UK) and Greiner Bio-One (Stonehouse, UK)

278   respectively. All XF assay consumables were purchased from Agilent Technologies (CA, USA). All

279   other reagents and chemicals were purchased from Sigma Aldrich (Dorset, UK) unless otherwise

280   stated.

281   *Cohort*

282   Ten healthy volunteers were recalled to give blood from the previously established HLA-typed

283   archive (Alfirevic et al. 2012). These volunteers were selected upon the basis of their mitochondrial

284   haplogroup (haplogroup H and J) and this genotyping has been described in our previous publication

285   (Ball *et al,* 2021). Mitochondrial subhaplogroups and SNPs of the DNA isolated from each individual

286   are described in the Supplementary Information. Ten donors were selected as an adequate number

287   for a proof of principle study on the feasibility of generating the transmitochondrial cybrids. The

288   volunteers were eligible to take part in the study if they were aged between 18 and 60 years,

289   healthy and willing to donate one or more blood samples. The following exclusion criteria were

290   applied and volunteers were not recruited if: they donated blood to transfusion services in the last 4

291   months; they had any medical problems, including asthma, diabetes, epilepsy or anemia; on any

292   medications or if they had taken any recreational drugs in the last 6 weeks (including cannabis,

293   speed, ecstasy, cocaine, LSD, and so on). Women were excluded if pregnant. This project was

294   approved by the North West of England Research Ethics Committee and all participants gave written

295   informed consent. Volunteer confidentiality was maintained by double coding DNA samples and by

296   restricting access to participant's personal data to trained clinical personnel. Detailed study eligibility

297   and exclusion criteria have been published previously (Alfirevic et al. 2012).

298

299   *Generation of HepG2 cybrids*

300   *Generation of HepG2 ρ0 cells*

301   HepG2 cells (ECACC Cat# 85011430, RRID:CVCL_0027) (≤ passage 7) were cultured and passaged as

302   required in HepG2 ρ0 cell medium (DMEM/F-12 +GlutaMAX^{TM} supplemented with FBS [10% v/v],

303   L-glutamine [4 mM], sodium pyruvate [1 mM], HEPES [2 mM] and uridine [500 µM]) in the presence

304   of ethidium bromide (EtBr; 1 μM). During treatment with EtBr (1 μM), the chemical was removed for

305   48 h every two weeks to help maintain cell viability. Following eight weeks' exposure, EtBr was

306   removed from a subset of cells for one week prior to characterisation to ensure cells were devoid of

307   mtDNA i.e. were ρ0 cells (see Supplementary Information). If a ρ0 cell phenotype was not evident,

308   cells were returned to EtBr treatment (1 μM) prior to removal for another week and re-testing, until

309   a ρ0 cell population was observed.

310   *Platelet isolation*

311   Healthy volunteers, five of mitochondrial haplogroup H, and five of haplogroup J, donated whole

312   blood from which platelets were isolated according to methods previously described (Ball et al.,

313   2021). Briefly, 50 mL of blood was donated by each volunteer, and this fresh whole blood was

314   immediately processed by a series of density centrifugation steps to produce isolated platelets.

315   Throughout the procedure, PGI_2 was used (1 μg/mL) to prevent platelet activation.

316   *Platelet fusion with HepG2 rho zero (ρ0) cells*

317   During the final centrifugation step of platelet isolation, HepG2 ρ0 cells were collected by

318   trypsinisation and resuspended in HepG2 ρ0 cell medium. Following cell viability assessment (trypan

319   blue; all viabilities were recorded at >90%), ρ0 cells (6 x 10^6 cells) were centrifuged (1000 g, 5 min)

320   and resuspended in Ca^{2+}-free DMEM (2 mL; supplemented with 1 mM PGI2). This cell suspension

321   was added to isolated platelets using a Pasteur pipette so as to minimise disruption to the platelet

322   pellet. The cell mixture was then centrifuged (180 g, no brake, 10 min) to form a multi-layered pellet

323   of platelets and HepG2 ρ0 cells.

324   Following centrifugation, the supernatant was removed and polyethylene glycol (250 μL; PEG 50%)

325   was added before resuspending the cell pellet (30 s) followed by a 1 min incubation period. At the

326   end of the incubation period, HepG2 ρ0 cell medium (30 mL) was added and a further 10-fold or 2-

327   fold dilution with HepG2 ρ0 cell medium was performed before seeding into 96-well, 12-well and 6-
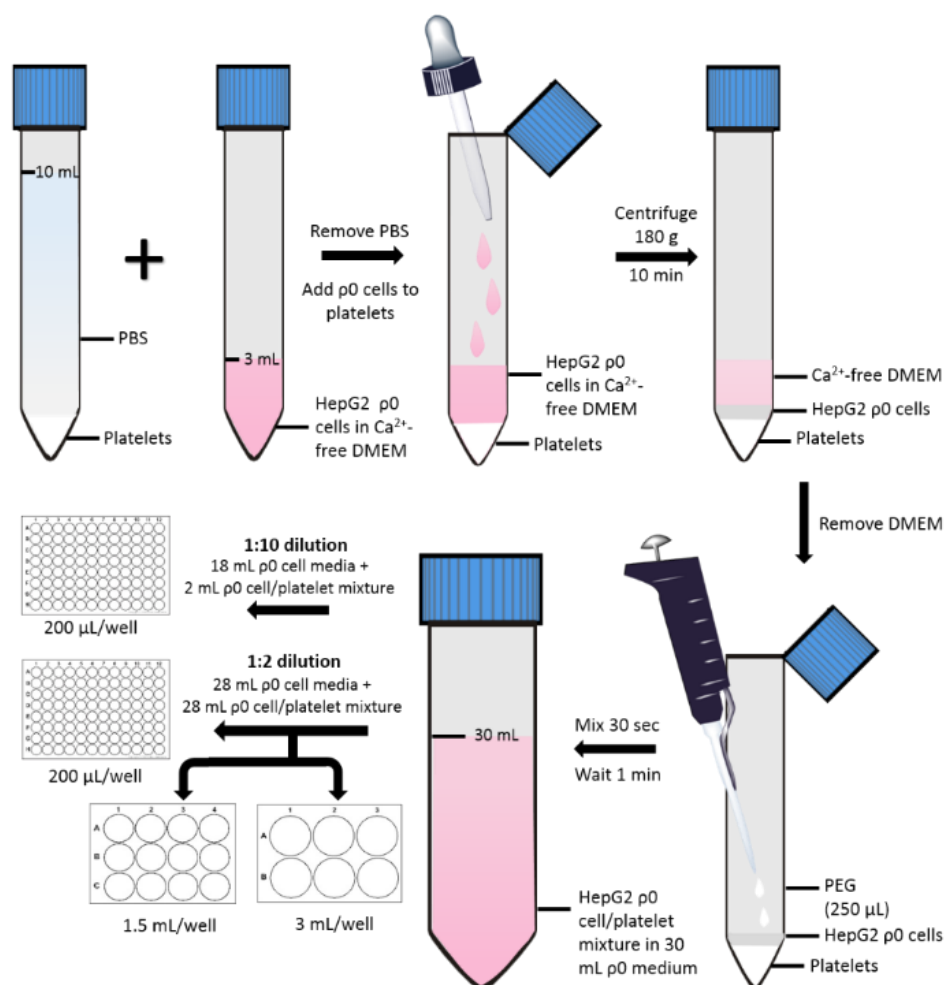
328   well plates (Figure 7)

329

Figure 7 Schematic representation of the fusion of HepG2 ρ0 cells and platelets to generate HepG2 transmitochondrial cybrids. HepG2 ρ0 cells were assessed for viability (trypan blue; all viabilities were recorded at >90%), 6×10^6 ρ0 cells were then centrifuged (1000 g, 5 min) and resuspended in Ca^{2+}-free DMEM (2 mL; supplemented with 1 mM PGI_2). This cell suspension was added to isolated platelets using a Pasteur pipette so as to minimise disruption to the platelet pellet. The cell mixture was then centrifuged (180 g, no brake, 10 min) to form a multi-layered pellet of platelets and HepG2 ρ0 cells. Following centrifugation, the supernatant was removed and polyethylene glycol (250 µL; PEG 50%) was added before resuspending the cell pellet (30 sec) followed by a 1 min incubation period. At the end of the incubation period, HepG2 ρ0 cell medium (30 mL) was added and a further 10-fold or 2-fold dilution with HepG2 ρ0 cell medium was performed before seeding into 96-well, 12-well and 6-well plates. Abbreviations: PEG, polyethylene glycol; ρ0, rho zero.

330 Two days post-fusion, media were replaced with fresh HepG2 ρ0 cell medium. After a further two

331 days, this was replaced with medium consisting of equal volumes of HepG2 ρ0 medium and cybrid

332 selection medium (high-glucose DMEM [glucose; 25 mM] supplemented with dialysed FBS [10% v/v],

333 amphotericin B [1.35 µM] and antibiotic/antimycotic solution [100 units penicillin/mL, 170 µM

334 streptomycin and 270 nM amphotericin B]). Finally, two days later, media were switched to 100%

335 cybrid selection medium. ρ0 cells are auxotrophic for pyruvate and uridine, so the absence of these

336 two constituents was the basis for the selection of successfully fused cells i.e. HepG2 cybrids. Cells

18

337   remaining after selection were characterised to ensure a HepG2 cybrid phenotype by measuring the

338   expression and function of mtDNA-encoded proteins (see Supplementary Information). Cells were

339   then cultured and passaged as required in cybrid maintenance medium (DMEM high-glucose

340   supplemented with FBS [10% v/v], L-glutamine [4 mM], sodium pyruvate [1 mM] and HEPES [1

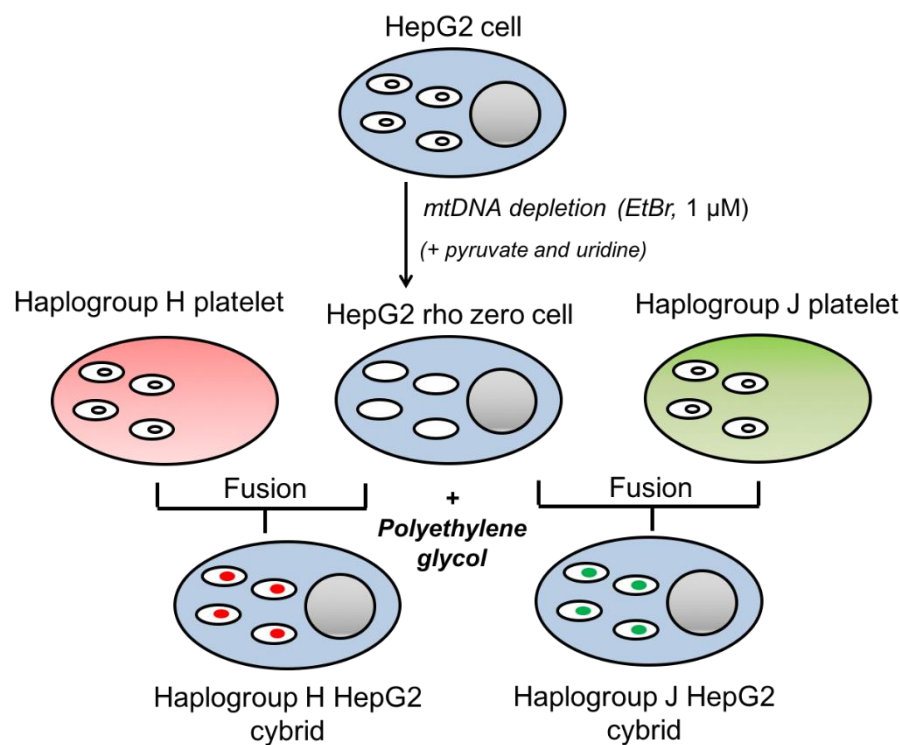341   mM]). For a schematic representation of HepG2 cybrid generation see Figure 8.

342

Figure 8 Schematic representation of HepG2 transmitochondrial cybrid generation. HepG2 cells were cultured in the presence of 1 μM ethidium bromide to generate HepG2 ρ0 cells. HepG2 ρ0 cells were combined with freshly-isolated platelets from healthy volunteers of mitochondrial haplogroup H or J and centrifuged (180 g, 10 min) to generate a multi-layered pellet. Following removal of the supernatant, polyethylene glycol (PEG; fusion reagent) was added and suspended with the cell mixture. After incubation with PEG for 1 min, 30 mL of HepG2 ρ0 cell medium was added (containing uridine and pyruvate) before further dilutions into a range of cell culture vessel sizes. This cell mixture was then cultured in cybrid selection medium (devoid of pyruvate and uridine), remaining cells were characterised to ensure the expression and function of mtDNA-encoded proteins. Abbreviations: EtBr, ethidium bromide; mtDNA, mitochondrial DNA.

343

344 *Assessment of mitochondrial function at basal state and following incubation with flutamide, 2-*
345 *hydroxyflutamide and tolcapone*

346 *Dual assessment of mitochondrial function (ATP content) alongside cytotoxicity (LDH release)*

347 *Cell and reagent preparation*

348 HepG2 cybrids were collected by trypsinisation and seeded on a collagen-coated flat-bottomed
349 96-well plate in cybrid maintenance medium (20 000 cells/50 µL/well) and incubated (24 h, 37°C, 5%
350 CO_2). Cells were then washed three times in serum-free galactose medium (DMEM containing 10
351 mM galactose and 6 mM L-glutamine) before addition of galactose medium (50 µL) and further
352 incubation (2 h, 37°C, 5% CO_2). This acute metabolic modification has been shown to be sufficient to
353 allow the identification of drugs which induce mitochondrial dysfunction, by reducing the ATP yield
354 from glycolysis, thereby increasing reliance on OXPHOS for ATP production. Flutamide, 2-
355 hydroxyflutamide, tolcapone, bicalutamide and entacapone were each serially diluted to generate a
356 concentration range of 0.01 – 300 µM in galactose medium. Diluted compounds (50 µL) were then
357 added to each well (total well volume; 100 µL) and cells were incubated (2 h, 37°C, 5% CO_2) before
358 conducting assays to assess mitochondrial function and cytotoxicity. All assays used ≤0.5% DMSO as
359 a vehicle control.

360 *ATP content assay*

361 ATP content was assessed by the addition of cell lysate (10 µL) and ATP standard curve solutions to a
362 white-walled 96-well plate. ATP assay mix (40 µL; prepared according to the manufacturer's
363 instructions) was then added and bioluminescence was measured (Varioskan, Thermo Scientific).

364 *LDH release assay*

365 LDH release was determined by the extraction of 25 µL supernatant and 10 µL cell lysate from each
366 well, before use of a cytotoxicity detection kit and reading at 490 nm. LDH release was calculated as:
367 LDH supernatant/ (supernatant + lysate).

368 *Normalisation (BCA assay)*

369 Protein content was determined using cell lysate (10 µL) and protein standards (10 µL). BCA assay
370 fluorescence was then measured at 570 nm.

371 *Extracellular flux analysis*

372 HepG2 cybrids were collected by trypsinisation and seeded on a collagen-coated XFe96 cell culture
373 microplate (25 000 cells/100 µL medium/well; 96-well plate) and incubated (37°C, 5% CO_2)
374 overnight.

375   *Mitochondrial stress test*

376   Please refer to Ball et al, 2016 for a detailed description of this method (Ball et al., 2016). Briefly,

377   cells were incubated (1 h, 37°C, 0% CO_2) before replacement of culture medium with 175 µL of

378   unbuffered Seahorse XF base medium supplemented with glucose (25 mM), L-glutamine (2 mM),

379   sodium pyruvate (1 mM), pre-warmed to 37°C (pH 7.4). Following an equilibration period,

380   measurements were taken to establish a baseline oxygen consumption rate (OCR) prior to the acute

381   injection of each of the five test compounds (7.8-500 µM). Following compound injection a

382   mitochondrial stress test consisting, of sequential injections of oligomycin (ATP synthase inhibitor; 1

383   µM), carbonyl cyanide 4-(trifluoromethoxy) phenylhydrazone (FCCP) (uncoupler; 0.5 µM) and

384   rotenone/antimycin A (complex I/III inhibitors respectively; 1 µM each), was performed.

385   *Respiratory complex assays*

386   Please refer to Salabei et al, 2014 for a detailed description of this method (Salabei et al., 2014).

387   Briefly, culture medium was replaced with mitochondrial assay solution buffer (MAS: $MgCl_2$; 5 mM,

388   mannitol; 220 mM, sucrose; 70 mM, KH_2PO_4; 10 mM, HEPES; 2 mM, EGTA; 1 mM, BSA; 0.4% w/v)

389   containing constituents to permeabilise cells and stimulate oxygen consumption via complex I (ADP;

390   4.6 mM, malic acid; 30 mM, glutamic acid; 22 mM, BSA; 30 µM, PMP; 1 nM), complex II (ADP; 4.6

391   mM, succinic acid; 20 mM, rotenone; 1 µM, BSA; 30 µM, PMP; 1 nM), complex III (ADP; 4.6 mM,

392   duroquinol; 500 µM, rotenone; 1 µM, malonic acid; 40 µM, BSA; 0.2% w/v, PMP; 1 nM) or complex

393   IV (ADP; 4.6 mM, ascorbic acid; 20 mM, TMPD (N,N,N',N'-tetramethyl-p-phenylenediamine); 0.5

394   mM, antimycin A; 2 mM, BSA; 30 mM, PMP; 1 nM). Following a basal measurement (no equilibration

395   period) of three cycles of mix (30 s), wait (30 s) and measure (2 min), flutamide or 2-

396   hydroxyflutamide (or MAS buffer for determination of basal complex activity) was injected followed

397   by a mitochondrial stress test as detailed previously, only each measurement cycle was 3 min rather

398   than 6 min.

399   *Statistical analysis*

400   In total 10 distinct cybrid cell lines were generated, one from each recruited volunteer, specifically 5

401   x distinct haplogroup H cell lines, and 5 x distinct haplogroup J cell lines. Additionally, 5 cybrid

402   populations were generated for each cell line (volunteer). Each population was tested as an

403   independent experiment (n =1), therefore giving a total of n=5 for each cybrid cell line/volunteer.

404   Each independent experiment contained a minimum of 3 technical replicates.

405   Platelets were provided to the investigator blinded to haplogroup, to avoid bias; therefore, cybrid

406   generation, experiments and subsequent data analyses were performed on cybrids for which the

21

407 haplogroup was unknown. Unblinding occurred at the stage at which datasets were combined to the

408 to enable the subsequent statistical comparison of haplogroup H vs haplogroup J.

409 Parameters for comparison were predefined to discourage statistical bias during analyses. These

410 were, for both the assessment of mitochondrial function and drug-induced mitochondrial

411 dysfunction: basal, maximum and ATP-linked respiration, spare respiratory capacity, proton leak and

412 complex I-IV activity. Normality was assessed using a Shapiro-Wilk test. All data were assessed as

413 parametric and therefore statistical significance was determined by an unpaired t-test using

414 GraphPad Prism Version 7.0. Significance was determined when p value <0.05. EC_{50} data were

415 determined by nonlinear regression analysis using GraphPad Prism 7.0 for the assessment of drug

416 treatment on ATP level.

References

418 Alfirevic A, Gonzalez-Galarza F, Bell C et al (2012) In silico analysis of HLA associations with drug-
419 induced liver injury: use of a HLA-genotyped DNA archive from healthy volunteers. Genome Med
420 4:51. doi: 10.1186/gm350.

421 Amuthan, G., Biswas, G., Ananadatheerthavarada, H.K., Vijayasarathy, C., Shephard, H.M., and
422 Avadhani, N.G. (2002). Mitochondrial stress-induced calcium signaling, phenotypic changes and
423 invasive behavior in human lung carcinoma A549 cells. Oncogene 21: 7839–7849. doi:
424 10.1038/sj.onc.1205983.

425 Bale, S.S., Vernetti, L., Senutovitch, N., Jindal, R., Hegde, M., Gough, A., et al. (2014). In Vitro
426 Platforms for Evaluating Liver Toxicity. Exp. Biol. Med. (Maywood). 239: 1180–1191. doi:
427 10.1177/1535370214531872.

428 Ball, A.L., Bloch, K.M., Rainbow, L., Liu, X., Kenny, J., Lyon, J.J., et al. (2021). Assessment of the impact
429 of mitochondrial genotype upon drug-induced mitochondrial dysfunction in platelets derived from
430 healthy volunteers. Arch. Toxicol. 1–13. doi: 10.1007/s00204-021-02988-3

431 Ball, A.L., Kamalian, L., Alfirevic, A., Lyon, J.J., and Chadwick, A.E. (2016). Identification of the
432 Additional Mitochondrial Liabilities of 2-Hydroxyflutamide When Compared With its Parent
433 Compound, Flutamide in HepG2 Cells. Toxicol Sci. doi: 10.1093/toxsci/kfw126.

434 Benabou, R., and Waters, C. (2003). Hepatotoxic profile of catechol-O-methyltransferase inhibitors
435 in Parkinson's disease. Expert Opin. Drug Saf. 2: 263–267. doi: 10.1517/14740338.2.3.263.

436 Bernal, W., and Wendon, J. (2013). Acute liver failure. N. Engl. J. Med. 369: 2525–2534. doi:
437 10.1056/NEJMra1208937.

438 Coe, K.J., Jia, Y., Ho, H.K., Rademacher, P., Bammler, T.K., Beyer, R.P., et al. (2007). Comparison of
439 the cytotoxicity of the nitroaromatic drug flutamide to its cyano analogue in the hepatocyte cell line
440 TAMH: evidence for complex I inhibition and mitochondrial dysfunction using toxicogenomic
441 screening. Chem Res Toxicol 20: 1277–1290. doi: 10.1021/tx7001349.

442 Dykens, J.A., and Will, Y. (2007). The significance of mitochondrial toxicity testing in drug
443 development. Drug Discov. Today 12: 777–785.

444   Eupedia (2016). European MtDNA Haplogroups Frequency.

445   Fermini, B., Coyne, K.P., and Coyne, S.T. (2018). Challenges in designing and executing clinical trials
446   in a dish studies. J. Pharmacol. Toxicol. Methods 94: 73–82. doi: 10.1016/j.vascn.2018.09.002.

447   Fontana, R.J. (2014). Pathogenesis of Idiosyncratic Drug-Induced Liver Injury and Clinical
448   Perspectives. Gastroenterology 146: 914–928. doi: 10.1053/j.gastro.2013.12.032.

449   Ghelli, A., Porcelli, A.M., Zanna, C., Vidoni, S., Mattioli, S., Barbieri, A., et al. (2009). The background
450   of mitochondrial DNA haplogroup J increases the sensitivity of Leber's hereditary optic neuropathy
451   cells to 2,5-hexanedione toxicity. PLoS One 4: e7922. doi: 10.1371/journal.pone.0007922.

452   Jones SW, Ball AL, Chadwick AE, Alfirevic A. The Role of Mitochondrial DNA Variation in Drug
453   Response: A   Systematic   Review.   Front   Genet.   2021a   Aug   17;12:698825.   doi:
454   10.3389/fgene.2021.698825.

455   Jones, S.W., Penman, S.L., French, N.S., Park, B.K., and Chadwick, A.E. (2021b). Investigating
456   dihydroorotate dehydrogenase inhibitor mediated mitochondrial dysfunction in hepatic in vitro
457   models. Toxicol. Vitr. 72: 105096. doi: 10.1016/j.tiv.2021.105096.

458   King, M.P., and Attardi, G. (1989). Human cells lacking mtDNA: repopulation with exogenous
459   mitochondria by complementation. Science (80-.). 246: 500–503. doi: 10.1126/science.2814477.

460   Lees, A.J. (2008). Evidence-based efficacy comparison of tolcapone and entacapone as adjunctive
461   therapy   in   Parkinson's   disease.   CNS   Neurosci.   Ther.   14:   83–93.   doi: 10.1111/j.1527
462   3458.2007.00035.

463   Leise, M.D., Poterucha, J.J., and Talwalkar, J.A. (2014). Drug-induced liver injury. Mayo Clin Proc 89:
464   95–106. doi: 10.1016/j.mayocp.2013.09.016.

465   Longo, D.M., Yang, Y., Watkins, P.B., Howell, B.A., and Siler, S.Q. (2016). Elucidating Differences in
466   the Hepatotoxic Potential of Tolcapone and Entacapone With DILIsym((R)), a Mechanistic Model of
467   Drug-Induced   Liver   Injury.   CPT   Pharmacometrics   Syst.   Pharmacol.   5:   31–39.   doi:
468   10.1002/psp4.12053.

469   Luo, Y., Bond, J.D., and Ingram, V.M. (1997). Compromised mitochondrial function leads to increased
470   cytosolic calcium and to activation of MAP kinases. Proc. Natl. Acad. Sci. 94: 9705–9710. doi:
471   10.1073/pnas.94.18.9705.

472   Olanow, C.W. (2000). Tolcapone and hepatotoxic effects. Tasmar Advisory Panel. Arch. Neurol. 57:
473   263–267. doi: 10.1001/archneur.57.2.263.

474   Olanow,   C.W.,   and   Watkins,   P.B.   (2007).   Tolcapone: an   efficacy   and   safety   review.   Clin.
475   Neuropharmacol. 30: 287–294. doi: 10.1097/wnf.0b013e318038d2b6.

476   Oven, M. Van, and Kayser, M. (2009). Updated comprehensive phylogenetic tree of global human
477   mitochondrial DNA variation. Hum Mutat 30(2):E386-94. doi: 10.1002/humu.20921.

478   Penman, S.L., Carter, A.S., and Chadwick, A.E. (2020). Investigating the importance of individual
479   mitochondrial genotype in susceptibility to drug-induced toxicity. Biochem. Soc. Trans. 48: 787–797.
480   doi: 10.1042/BST20190233.

481   Rivest, J., Barclay, C.L., and Suchowersky, O. (1999). COMT inhibitors in Parkinson's disease. Can. J.
482   Neurol. Sci. 26 Suppl 2: S34-8. doi: 10.1017/s031716710000007x.

483 Salabei, J.K., Gibb, A.A., and Hill, B.G. (2014). Comprehensive measurement of respiratory activity in
484 permeabilized cells using extracellular flux analysis. Nat. Protoc 9: 421–438. doi:
485 10.1038/nprot.2014.018.

486 Shet, M.S., McPhaul, M., Fisher, C.W., Stallings, N.R., and Estabrook, R.W. (1997). Metabolism of the
487 antiandrogenic drug (Flutamide) by human CYP1A2. Drug Metab. Dispos 25: 1298–1303.

488 Sison-Young, R.L., Mitsa, D., Jenkins, R.E., Mottram, D., Alexandre, E., Richert, L., et al. (2015).
489 Comparative Proteomic Characterization of 4 Human Liver-Derived Single Cell Culture Models
490 Reveals Significant Variation in the Capacity for Drug Disposition, Bioactivation, and Detoxication.
491 Toxicol Sci 147: 412–424. doi: 10.1093/toxsci/kfv136.

492 Srinivasan, S., Guha, M., Dong, D.W., Whelan, K.A., Ruthel, G., Uchikado, Y., et al. (2015). Disruption
493 of cytochrome c oxidase function induces the Warburg effect and metabolic reprogramming.
494 Oncogene. doi: 10.1038/onc.2015.227.

495 Tujios, S.R., and Lee, W.M. (2018). Acute liver failure induced by idiosyncratic reaction to drugs:
496 challenges in diagnosis and therapy. Liver Int. 38: 6–14. doi: 10.1111/liv.13535.

497 Watkins, P. (2000). COMT inhibitors and liver toxicity. Neurology 55: S51-2; discussion S53-6.

498 Wilkins, H.M., Carl, S.M., and Swerdlow, R.H. (2014). Cytoplasmic hybrid (cybrid) cell lines as a
499 practical model for mitochondriopathies. Redox Biol. 2: 619–631. doi: 10.1016/j.redox.2014.03.006.

500 Article and Author Information

507 **Authors' contributions:** Author A.L.B generated the cybrid models, contributed to study design,
508 completed laboratory work and data analysis, and wrote the manuscript. Author C.E.J contributed
509 towards the generation of cybrid models and study design, and provided critical feedback. Author J.J
510 contributed towards project conceptualisation. Author A.A contributed to funding acquisition,
511 project conceptualisation and securement of resources including collaboration with the Royal
512 Liverpool Research Facility. Author A.E.C acquired funding, conceptualised the project, directed data
513 analysis and provided critical feedback. All authors have approved the final manuscript.

514 **Competing interests:** JJL is affiliated with GSK GlaxoSmithKline. The other authors declare no
515 competing interests that pertain to this work.

516 **Ethics approval statement:** All procedures performed in studies involving human participants were
517 in accordance with the ethical standards of the North West of England Research Ethics Committee

518   (Cell Archive of HLA Typed Healthy Volunteers (HLA), CRN ID 7787, IRAS ID: 15623) with the 1964

519   Helsinki declaration and its later amendments or comparable ethical standards.

520   **Data availability:** Source data are provided as files linked to the appropriate table/figures.

521   Supplementary Information

522   *Mitochondrial DNA (MtDNA) variation of 10 healthy volunteers whose platelets were used to generate*
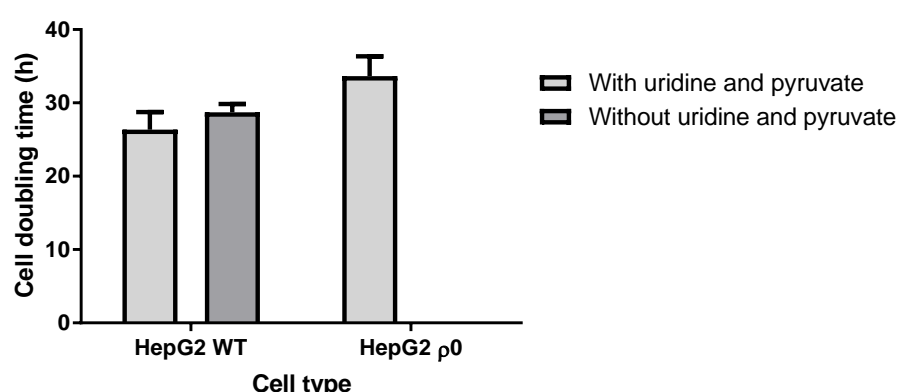523   *cybrids*

Donor	Haplogroup	Subhaplogroup	SNPs characteristic of assigned haplogroup	Additional SNPs
1	H	H1c3	257G 263G 477C 750G 1438G 3010A 4769G 8473C 8860G 15326G	195C 12966T 16519C
2	H	H1bb	152C 263G 750G 1438G 3010A 4769G 8860G 11864C 15326G	16519C
3	H	H1a1	73G 263G 750G 1438G 3010A 4769G 6365C 8860G 15326G 16162G	152C 3483A 16360T 16519C
4	H	H1c	263G 477C 750G 1438G 3010A 4769G 8860G 15326G	10646A 16519C
5	H	H2a1e1a1	263G 575T 750G 751G 951A 8860G 15326G 16124C 16148T 16166G 16354T	
6	J	J2b1g	73G 150T 152C 263G 489C 750G 1438G 4769G 5633T 7028T 8860G 9872G 10172A 10398G 11251G 11719A 12612G 13708A 14766T 15257A 15326G 15452A 15812A 16069T 16126C 16193T	2789T 13821T
7	J	J1c+16261	73G 185A 228A 263G 295T 462T 489C 750G 1438G 3010A 4216C 4769G 7028T 8860G 10398G 11251G 11719A 12612G 13708A 14766T 14798C 15326G 15452A 16069T 16126C 16261T	4113A 6554T 10915C 16316G
8	J	J1c1c	185A 228A 462T 482C 489C 750G 1438G 3010A 3394C 4216C 4769G 7028T 8860G 10398G 11251G 11719A 13708A 14766T 14798C 15326G 15452A 16069T 16126C 16145A	188G 13943T 14552G
9	J	J1c2h	185A 188G 222T 228A 263G 295T 462T 489C 750G 1438G 3010A 4216C 4769G 7028T 8860G 10398G 11251G 11719A 12612G 13708A 14766T 14798C 15326G 15452A 16069T 16126C	16189C 16519C 16527T
10	J	J1c1e	185A 228A 263G 295T 462T 482C 489C 750G 1438G 3010A 3394C 4216C 4769G 7028T 8860G 10398G 10454C 11251G 11719A 12612G 13708A 14766T 14798C 15326G 15452A 16069T 16126C 16368C	13889A

524   Additional SNPs refers to SNPs that were present in the sample but were not characteristic of the assigned haplogroup.
525   Abbreviations: SNP, single nucleotide polymorphism.

526

Characterisation of HepG2 rho zero cells and HepG2 transmitochondrial cybrids

528

529 <u>S1: Cell doubling time</u>

530 The dependence of HepG2 ρ0 cells on pyruvate and uridine meant that culture media devoid of

531 these constituents was able to select for the successful depletion of mtDNA and the resultant non-

532 functional electron transport chain in EtBr-treated cells. Concordantly, HepG2 WT cells had a similar

533 doubling time in media with or without these additives, averaging 26.2 hours. In contrast, HepG2 ρ0

534 cells exhibited no growth without uridine and pyruvate and an average doubling time of 27.6 hours

535 when in media containing these two constituents.

536 **Cell doubling time of HepG2 wild-type (WT) and HepG2 rho zero (ρ0) cells.** The two cell types were cultured in media with

537 or without uridine and pyruvate and growth rate calculated. Data are presented as mean+SEM of n=3 experiments. Source

538 data: figs s1 – source data file.xslx

539 <u>S2: Mitochondrial DNA content</u>

540 The Ct value of both mtDNA primers increased dramatically in ρ0 compared to WT cells whilst

541 nuclear DNA Ct values remained consistent across all three cell lines. Similarly, both HepG2 WT and

542 cybrid cells had thousands of mtDNA copies/cell in contrast to the ρ0 cells which had less than one

543 copy/cell

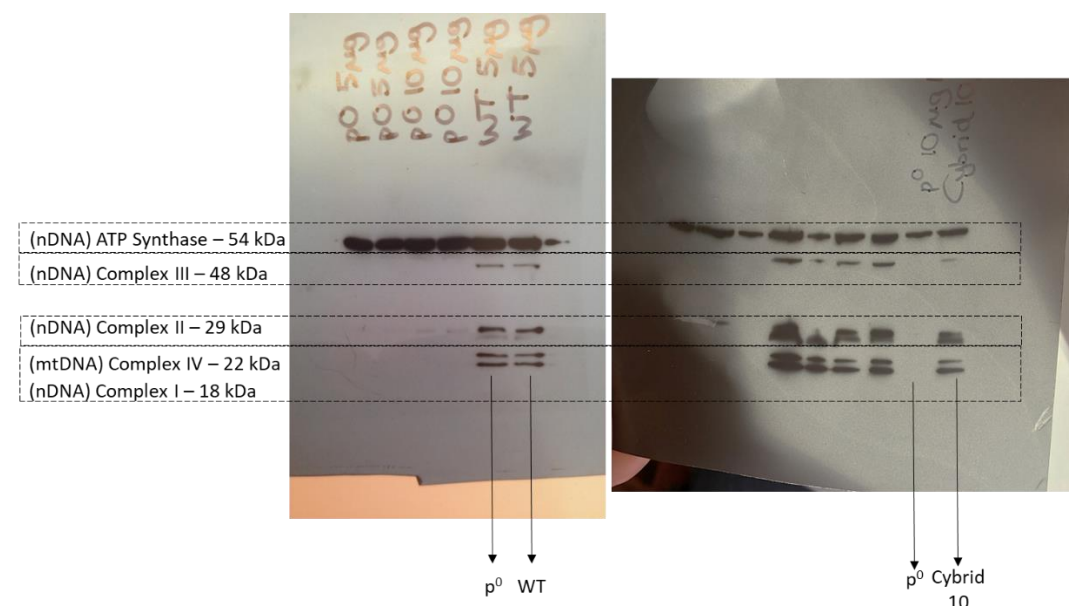544 **Assessment of mtDNA content in HepG2 wild-type (WT), HepG2 rho zero (ρ0) and HepG2 cybrids.**

Sample	Primer C_t value				mtDNA copies/cell			
	TERT	RNase P	ND-1	Custom	TERT/ ND-1	TERT/ custom	RNase P/ ND-1	RNase P/ custom
HepG2 WT	30.6 (1.00)	31.3 (1.11)	18.5 (0.120)	18.9 (0.140)	9280	6985	14563	10960
HepG2 ρ0	27.7 (0.0600)	27.2 (0.0700)	34.7 (0.740)	32.0 (0.180)	0.00400	0.0240	0.00300	0.0170
HepG2	29.8 (1.10)	30.4 (0.550)	18.9 (0.730)	19.0 (0.0900)	3875	3590	5673	5256

cybrid								

545   Abbreviations: C_t, cycle threshold; ND-1, NADH dehydrogenase-1; RNase, ribonuclease P RNA component H1; TERT,

546   telomerase reverse transcriptase; WT, wild-type; ρ0, rho zero. C_t values are displayed as mean (SEM).

547   *S3: Detection of mitochondrial/nuclear DNA-encoded mitochondrial proteins*

548   Western blot analysis showed expression of all nuclear DNA and mtDNA-encoded subunits of the

549   electron transport chain which were probed for in HepG2 WT and cybrid cells. However, ρ0 cells did

550   not express the mtDNA-encoded subunit of complex IV. Notably, despite all the other subunits being

551   encoded in the nuclear DNA, it was only the alpha subunit of ATP synthase that was retained in the

552   ρ0 cells.

553
554   **Representative western blots of HepG2 wild-type (WT), rho zero and cybrid cell lysates.** 10 µg of lysate protein was

555   resolved by SDS-PAGE and probed for subunits of complexes I (NDUFB8), II (Iron-sulphur protein (IP) 30 KDa), III (Core 2), IV

556   (II), V (alpha). Abbreviations: mtDNA, mitochondrial DNA; nDNA, nuclear DNA. Source data: figs s3 and s4 source data

557   file.xslx and figs s3 –raw data.pptx

558

559   *S4: Detection of electron transport chain function*

560   HepG2 WT and cybrid cells exhibited a classic response to the series of mitochondrial inhibitors used

561   to perform the mitochondrial stress test whereas the ρ0 cells did not respond to these inhibitors and

562   had very low basal OCR, all of which was due to non-mitochondrial respiration. The PPRgly /OCR

563   ratio was also higher in WT and ρ0 cells compared with cybrid cells.

564   **Differences in parameters of mitochondrial function in HepG2 wild-type (WT), rho zero (ρ0) and cybrid cells.**

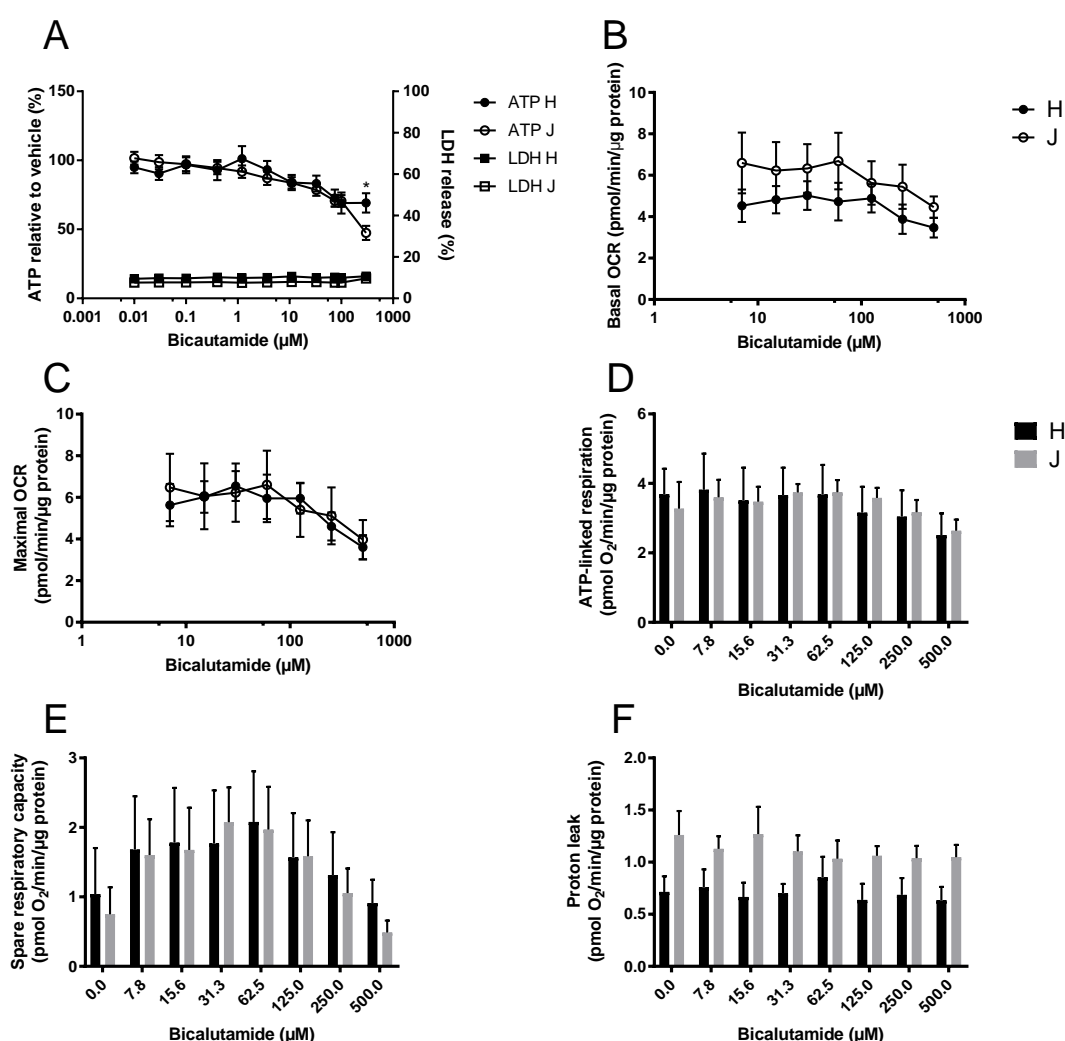| HepG2 cell type	Basal OCR (pmol/min/µg protein)	PPR_{gly}/OCR	% Non-mitochondrial respiration
WT	6.52 (0.350)	0.354 (0.0900)	28.4 (0.310)

27

Rho zero	0.450 (0.100)	55.5 (0.930)	102 (4.33)
Cybrid	6.53 (0.400)	0.466 (0.660)	24.3 (0.510)

565 Abbreviations: OCR, oxygen consumption rate; PPR$_{gly}$, proton production rate attributed to glycolysis; WT, wild-type.

566 Values are displayed as mean (SEM). Source data: figs s3 and s4 source data file.xslx

567 _S5: The effect of bicalutamide upon haplogroup H and J transmitochondrial cybrids_

568 Bicalutamide-treated cybrids of each haplogroup exhibited a similar decline in ATP content

569 until the highest concentration used (300 μM), when haplogroup J cybrids had significantly

570 less ATP (Figure A). As with flutamide and 2-hydroxyflutamide treatment, the decline in ATP

571 was in the absence of significant LDH release. No significant differences were evident

572 between the two cybrids groups in parameters of mitochondrial function using XF analysis,

573 however as was the case with flutamide and 2-hydroxyflutamide, haplogroup J exhibited

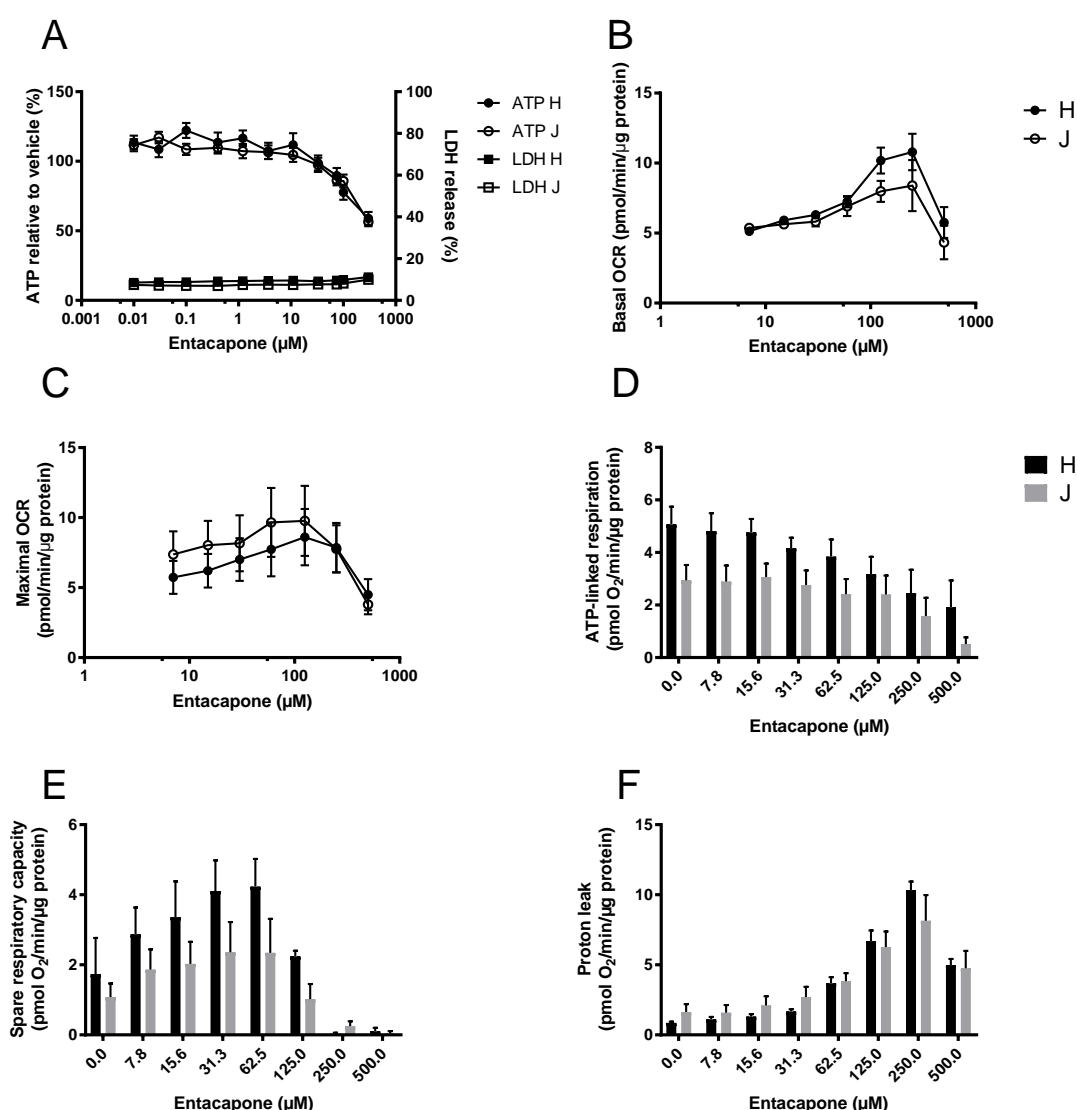574 higher proton leak in both control and treated cybrids (Figure B-F).

575 **The effect of bicalutamide upon ATP levels and mitochondrial respiratory function in haplogroup H and J HepG2 cybrids.**

576 **A:** Cybrids were treated (2 h) up to 300 μM bicalutamide in galactose medium. ATP values are expressed as a percentage of

577   those of the vehicle control. Lactate dehydrogenase (LDH) release is expressed as extracellular LDH as a % of total LDH. **B-F:**

578   XF analysis-detected changes in basal and maximal respiration, ATP-linked respiration, spare respiratory capacity and

579   proton leak following acute treatment with bicalutamide (up to 500 µM). Statistical significance between haplogroup H and

580   J cybrids: * $p<0.05$. Data are presented as mean ± SEM of n = 5 experiments. Source data: figs s5 – source data file.xslx

581

582   _S6: The effect of entacapone upon haplogroup H and J transmitochondrial cybrids_

583   Entacapone induced a weaker decline in ATP levels compared to tolcapone (Figure A). There

584   was no significant difference in ATP levels between the two haplogroups and also no

585   significant difference in parameters of mitochondrial function, though haplogroup H cybrids

586   had consistently higher ATP-linked respiration and spare respiratory capacity which tended

587   towards significance (Figure D, E).

588
589   **The effect of entacapone upon ATP levels and mitochondrial respiratory function in haplogroup H and J HepG2**

590   **transmitochondrial cybrids. A:** Cybrids were treated (2 h) with serial concentrations up to 300 µM entacapone in galactose

29

591   medium. ATP values are expressed as a percentage of those of the vehicle control. Lactate dehydrogenase (LDH) release is

592   expressed as extracellular LDH as a % of total LDH. **B-F:** Changes in basal respiration, maximal respiration, ATP-linked

593   respiration, spare respiratory capacity and proton leak following acute treatment with entacapone (up to 500 µM). Data

594   are presented as mean ± SEM of n = 5 experiments. Source data: figs s6 – source data file.xslx

595   ## Appendix: Supplementary Methods

596

597   *Methodology*

598   *Cell doubling time*

599   HepG2 wild-type (WT) cells and HepG2 rho zero (ρ0) cells were seeded at 30 000 cells/well in a

600   24-well plate in either ρ0 cell media (contains pyruvate and uridine) or selection media (devoid of

601   pyruvate and uridine). On days 1, 3, 5 and 7 of culture, cells were collected by trypsinisation and

602   counted, following which growth rate was calculated. Rho zero cells are auxotrophic for pyruvate

603   and uridine, but WT cells are not, therefore the absence of cell growth in selection media indicated

604   complete loss of mtDNA.

605   *DNA extraction and real-time PCR*

606   DNA extraction from HepG2 WT, HepG2 ρ0 and HepG2 cybrid cells was performed using a DNA mini

607   kit (Qiagen, Manchester, UK) according to the manufacturer's instructions. Sample DNA

608   concentrations and quality were then quantified using a Quant-iT^{TM} PicoGreen^{TM} dsDNA Assay Kit

609   and nanodrop spectrophotometry respectively (Fischer Scientific, Loughborough, UK).

610   Real-time PCR was carried out using two primers for regions of mtDNA; a custom sequence and ND-

611   1 (complex I subunit) and two primers for regions of nuclear DNA; telomerase reverse transcriptase

612   (TERT) and RNase P (Applied Biosystems, California, USA) (Malik et al., 2011).

613   **Real-time PCR primers used to amplify regions of mitochondrial and nuclear DNA.**

Gene	Dye/probe	Additional information
RNase P (nDNA)	VIC® dye-labelled TAMRA^{TM} probe	Location: chromosome 14, cytoband 14q11.2
TERT (nDNA)	VIC® dye-labelled TAMRA^{TM} probe	Location: chromosome 5, cytoband 5p15.33
Custom sequence (mtDNA)	FAM® dye-labelled MGB probe	Oligonucleotide sequences: **hmito F5** CTTCTGGCCACAGCACTTAAAC **hmito R5** GCTGGTGTTAGGGTTCTTTGTTTT
ND-1 (mtDNA)	FAM® dye-labelled MGB probe	Location: mtDNA 3307-4262

614   Abbreviations: FAM, carboxyfluorescein; MGB, minor groove binder; ND-1, NADH dehydrogenase-1; mtDNA, mitochondrial

615   DNA; TAMRA, 6-carboxytetramethyl-rhodamine; TERT, telomerase reverse transcriptase; VIC, 2'-chloro-7'phenyl-1,4-

616   dichloro-6-carboxy-fluorescein.

617   During sample preparation, 2X Taqman® genotyping master mix (5 μL), a nuclear DNA primer (0.5

618   μL), mtDNA primer (0.5 μL), dH$_2$0 (2 μL) and 10 ng DNA (2 μL) from each sample were combined to

619   give a final sample concentration of 1 ng/μL in each well. Real-time PCR was then carried out using

620   the viiA7 RT-PCR system (Life Technologies, UK). MtDNA copies per cell were calculated on the basis

621   that each nuclear DNA primer was present in diploid copies per cell and used the following formula,

622   where x_1= nuclear DNA primer cycle threshold (C_t) value, x_2=mtDNA primer C_t value: mtDNA copies

623   per cell = $2(2^{(x_1 - x_2)})$ (Schäfer, 2016).

624   *Detection of mitochondrial/nuclear DNA-encoded mitochondrial proteins*

625   HepG2 ρ0, HepG2 WT or HepG2 cybrid cells were lysed using sonication and 10 μg of lysate protein

626   was resolved by sodium dodecyl sulphate-polyacrylamide *gel* electrophoresis (SDS-PAGE) using 4-

627   12% Bis-Tris gel (Invitrogen, UK) in MOPS buffer (MOPS; tris-base; 1.21% w/v, sodium dodecyl

628   sulphate; 0.20% w/v, EDTA; 0.06% w/v in distilled water (dH$_2$0)).

629   This gel was then transferred to a nitrocellulose membrane (GE Healthcare, Buckinghamshire, UK) in

630   transfer buffer (tris-base; 0.30% w/v, glycine; 1.5% w/v, methanol; 20% v/v in dH$_2$0) and blocked

631   using 10% non-fat dried milk in Tris Buffered Saline-Tween (TBS-T: TBS; 0.50% v/v, tween; 0.10% v/v

632   in dH$_2$0).

633   Blocking solution was removed using TBS-T and the membrane probed for CI-20, CII-30, CIII-core2,

634   CIV-I and CV-alpha subunits of complexes I-V of the electron transport chain using MitoProfile® Total

635   OXPHOS Human WB Antibody Cocktail (Abcam, Cambridgeshire, UK) (0.20% v/v in 10% non-fat dried

636   milk in TBS-T). This was followed by anti-mouse secondary antibody (0.01% v/v in 10% non-fat dried

637   milk in TBS-T) before visualisation using an ECL™ system (GE Healthcare, Buckinghamshire, UK).

638   *Detection of electron transport chain function*

639   Mitochondrial stress tests were performed on untreated HepG2 WT, ρ0 and HepG2 cybrid cells using

640   extracellular flux analysis as described in the main text.

641   Extracellular flux analysis produced two raw outputs, oxygen consumption rate and extracellular

642   acidification rate (ECAR). ECAR can be indicative of the glycolytic rate of the cell, however it also

643   takes into account changes in ECAR due to oxidative phosphorylation. Therefore the measure of

644   PPR$_{gly}$, glycolytic production rate was used to quantify glycolysis, this was calculated by subtracting

645   respiratory acidification contributions from the total proton production rate.

$$PPR_{gly} = PPR_{tot} - PPR_{resp}$$

646   *Where*

$$PPR_{tot} = \frac{ECAR}{BP} \; and \; PPR_{resp} = \left(\frac{10^{pH-6.093}}{1 + 10^{pH-6.093}}\right)\left(\frac{\max H^+}{O_2}\right)(OCR_{tot} - OCR_{rot})$$

647   **Equations for the calculation of PPR$_{gly}$ from mitochondrial stress tests.** Abbreviations: PPR$_{gly}$, proton

648   production rate attributed to glycolysis; PPR$_{resp}$, proton production rate attributed to respiration; PPR$_{tot}$, total

649   proton production rate; ECAR, extracellular acidification rate; BP, buffering power; max H$^+$/O$_2$, derived

650   acidification for metabolic transformation of glucose oxidation; OCR$_{tot}$, total oxygen consumption rate; OCR$_{rot}$,

651   oxygen consumption rate following rotenone injection (Kelly, 2018).

652   *Appendix References*

653   Kelly, R. (2018). Biochemical Thermodynamic Modelling of Cellular Bioenergetics: A Quantitative
654   Systems Pharmacology Approach. Liverpool John Moores University.

655   Malik, A.N., Shahni, R., Rodriguez-de-Ledesma, A., Laftah, A., and Cunningham, P. (2011).
656   Mitochondrial DNA as a non-invasive biomarker: Accurate quantification using real time quantitative
657   PCR without co-amplification of pseudogenes and dilution bias. Biochem. Biophys. Res. Commun.
658   412: 1–7.

659   Schäfer, I. University of Leipzig (2016). Personal Communication.

660

661